Crystal and Molecular Structure of [$SnLCl_3$]. The Single-crystal Electron Paramagnetic Resonance Spectra of [$MoE(L)Cl_2$] and [$MoO(L)(NCS)_2$] diluted in [$SnLCl_3$] [E = O or S; L = tris(3,5-dimethylpyrazolyl)hydroborate] †

David Collison,[a] David R. Eardley,[a] Frank E. Mabbs,*[,a] Keith Rigby,[a] Michael A. Bruck,[b] John H. Enemark[b] and Pamela A. Wexler[b]

[a] *Department of Chemistry, University of Manchester, Manchester M13 9PL, UK*

[b] *Department of Chemistry, University of Arizona, Tucson, AZ 85721, USA*

The crystal structure of [$SnLCl_3$] has been determined and shown to consist of discrete distorted *fac*-octahedral molecules [L = tris(3,5-dimethylpyrazolyl)hydroborate]. The single-crystal EPR spectra, at room temperature and Q-band frequencies, of [$MoE(L)Cl_2$] and [$MoO(L)(NCS)_2$], E = O or S, diluted in the structurally similar [$SnLCl_3$] have been recorded. The data from the different possible diluent sites in [$SnLCl_3$] are consistent with exact, or nearly exact, monoclinic EPR symmetry for each of the molybdenum compounds which involves a rotation of the *g* and *A* tensors about an axis perpendicular to the mirror plane in each molecule. The angles of rotation are in the range 30–38° and are in good agreement with those obtained *via* simulation of the frozen-solution X-band EPR spectra of the compounds. The relationships between the *g* and *A* tensors, the molecular geometries, and the electronic structures are discussed.

As part of our work on the chemical, structural and electronic properties of compounds of the early d-transition elements we have an interest in the relationship between the *g* and metal *A* tensors and the geometry, particularly of low-symmetry species. In low symmetry there may be non-coincidence of the principal axes of the *g* and *A* tensors. In addition these tensor axes may not coincide with any metal–ligand directions. Non-coincidence between the *g* and *A* tensors can sometimes be detected and measured from frozen-solution EPR spectra. We have previously reported such measurements on the compounds [$MoE(L)X_2$], where L = tris(3,5-dimethylpyrazolyl)hydroborate, E = O and X = Cl, NCS, OMe, or SEt,[1] and E = S and X = Cl.[2] This group of molecules have, or closely approximate to, C_s point symmetry. For this point symmetry one of the principal *g* and *A* tensor axes is required to be mutually coincident and perpendicular to the mirror plane, whilst the others are rotated relative to each other by an angle α_t. In this group of molecules simulation of frozen-solution spectra gave values of α_t which varied between 27° when X = NCS and 39° when X = SEt. Whilst the frozen-solution studies yield the values and relative orientations of the *g* and *A* tensors, single-crystal studies are required both to confirm these deductions and to determine their orientations with respect to the atomic framework.

Although many monomeric oxomolybdenum(v) compounds are known, relatively few detailed single-crystal EPR studies have been performed because of the lack of suitable diamagnetic host lattices. Following our successful use[3,4] of the pseudo-isostructural relationship $[VO]^{2+} \equiv [MCl]^{2+}$, where M = Ga or In, we have explored the use of a similar relationship, *viz.* $[LMoO]^{2+} \equiv [LSnCl]^{2+}$. Thus we now report the single-crystal structure determination of [$SnLCl_3$] and its use as a diamagnetic diluent in single-crystal EPR studies of [$MoO(L)X_2$], X = Cl or NCS and [$MoS(L)Cl_2$]. These results will be contrasted with those for [$VO(L)(S_2CNR_2)$], where S_2CNR_2 = dialkyldithiocarbamate. Preliminary results for EPR studies on [$SnLCl_3${MoO}] have been reported.[5]

† *Supplementary data available:* see Instructions for Authors, *J. Chem. Soc., Dalton Trans.*, 1994, Issue 1, pp. xxiii–xxviii.

Experimental

Preparations.—The molybdenum compounds were prepared as reported previously.[2,6] Potassium tris(3,5-dimethylpyrazolyl)hydroborate (KL) was prepared by the literature method.[7] The compound [$SnLCl_3$] was prepared by adding $SnCl_4$ (0.5 cm^3, 4.27 mmol) to a stirred solution of KL (1.47 g, 4.39 mmol) in dichloromethane. The mixture was filtered immediately and the clear filtrate evaporated *in vacuo* to produce a white powder. The powder was washed with methanol to remove any KCl. Colourless hexagonal-shaped crystals of [$SnLCl_3$] were obtained by recrystallisation from dichloromethane (Found: C, 34.7; H, 4.6; Cl, 20.1; N, 15.8; Sn, 20.1. Calc. for $C_{15}H_{22}BCl_3N_6Sn$: C, 34.50; H, 4.20; Cl, 20.40; N, 16.10; Sn, 22.75%).

Crystal Growth.—Pale green hexagonal prisms of [$MoO(L)Cl_2$] (1.5% Mo by analysis) in [$SnLCl_3$] were obtained by slow evaporation of a dichloromethane solution containing [$SnLCl_3$] and [$MoO(L)Cl_2$] in a ratio of 100:1. Deep pink hexagonal prisms of [$MoO(L)(NCS)_2$] (0.2% Mo by analysis) in [$SnLCl_3$] were produced by slow evaporation of a *dried* dichloromethane solution containing [$SnLCl_3$] and [$MoO(L)(NCS)_2$] in a ratio of 100:1. The evaporation was performed in a glove-box in an atmosphere of dry dinitrogen. Small yellow hexagonal prisms of [$MoS(L)Cl_2$] (2.8% Mo by analysis) in [$SnLCl_3$] were produced by rapid evaporation of a *dried* dichloromethane solution of [$SnLCl_3$] and [$MoS(L)Cl_2$] in a ratio of 65:1. The sulfido compound is sensitive to hydrolysis and to oxidation, thus a small amount of B_2S_3 was suspended in the solution and the evaporation took place in an atmosphere of dried dinitrogen.

Crystal Structure Determination of [$SnLCl_3$].—*Data collection.* The determination of the Bravais lattice, cell dimensions,

and the collection of intensity data were carried out on a Syntex $P2_1$ diffractometer equipped with a graphite monochromator. A crystal was mounted on a glass fibre in a random orientation and the cell constants and an orientation matrix for data collection were obtained from least-squares refinement using the setting angles of 25 reflections in the range $20 < 2\theta < 30°$. Data collection, intensity measurement and refinement parameters are summarised in Table 1. As a check on crystal quality, ω scans of several intense reflections were measured; the width at half-height was 0.20°, indicating good crystal quality. From the systematic absences of $0k0, k = 2n$, and from subsequent least-squares refinement, the space group was determined to be $P2_1/m$ (no. 11).

The variable scan rate used allowed rapid data collection for intense reflections at a fast scan rate, and assured good counting statistics for weak reflections at a slow scan rate. The scan range (°) was determined as a function of 2θ to correct for the separation of the Kα doublet. The ratio of peak counting time to background counting time was 2.0:1.

Data reduction. As a check on crystal and electronic stability, two check reflections were measured after every 98 data reflections. The intensities of these standards remained constant within experimental error throughout data collection and no decay correction was applied. An empirical absorption correction was made using the method described by Walker and Stuart,[8] with correction factors on I ranging from 0.748 to 1.226. Intensities of equivalent reflections were averaged. The agreement factor for the averaging of the 259 observed and accepted reflections was 0.009 based on intensity and 0.007 based on F_o. No corrections were made for extinction.

Structure solution and refinement. The structure was solved using the Patterson heavy-atom method which revealed the position of the Sn atom. The remaining atoms were located in succeeding Fourier-difference syntheses. Hydrogen atoms were located and added to the structure-factor calculation, but their positions were not refined. The structure was refined by full-matrix least-squares, where the function minimised was $\Sigma w(|F_o| - |F_c|)^2$. The least-squares weights for each reflection were calculated using the counter weighting scheme in Table 1. Scattering factors were taken from Cromer and Waber.[9] Anomalous dispersion effects[10] for all non-hydrogen atoms were included in F_c; the values for $\Delta f'$ and $\Delta f''$ were those of Cromer.[11] Only the 1822 reflections having intensities greater than 3.0 times their standard deviation were used in the refinements. The final cycle of refinement included 133 variable parameters and the refinement converged (largest parameter shift was less than 0.005 times its e.s.d.) with $R = 0.022$ and $R' = 0.037$ (inclusion of all the data gave $R = 0.025$ and $R' = 0.038$). Only the three correlation coefficients between the overall scale factor and U_{ii} of the Sn atom were greater than 0.50, the largest being 0.66 between the scale factor and U_{11}. The highest peak in the final difference electron-density map had a height of 0.46(6) e Å^{-3}.[12] Plots of $\Sigma w(|F_o| - |F_c|)^2$ *versus* $|F_o|$, reflection order in data collection, $(\sin\theta)/\lambda$, and various classes of indices showed no unusual trends. All calculations were performed on a Vax computer using SPD/VAX.[13]

Additional material available from the Cambridge Crystallographic Data Centre comprises H-atom coordinates, thermal parameters and remaining bond lengths and angles.

EPR Spectroscopy.—First-derivative EPR spectra were obtained at X- and Q-band frequencies using a Varian E112 spectrometer. Spectra at room temperature and Q-band frequencies on oriented single crystals of $[MoO(L)Cl_2]$, $[MoO(L)(NCS)_2]$, and $[MoS(L)Cl_2]$ diluted in $[SnLCl_3]$, and on powdered samples of these materials at both X- and Q-band frequencies, were obtained. The unit-cell parameters for the diluted crystals were within 1% of those for the pure host. Measurements were obtained on $[SnLCl_3\{MoO\}]$ and $[SnLCl_3\{MoS\}]$ with respect to the a^*b, a^*c, and bc crystal planes, whilst those for $[SnLCl_3\{MoO(NCS)_2\}]$ were with respect to the ab, ac^*, and bc^* planes. The spectra were treated, as we have reported previously,[14] by methods similar to those of Schonland,[15] and of Lund and Vånngard.[16]

Results and Discussion

Crystal Structure.—The atomic positional parameters for the non-hydrogen atoms are in Table 2. The structure consists of discrete six-co-ordinate pseudo-octahedral $[SnLCl_3]$ molecules, see Fig. 1 for the atomic numbering. The molecule has crystallographic mirror symmetry, with the mirror plane perpendicular to the b axis and containing Sn, Cl(1), B, and the pyrazole ring defined by N(21), N(22), C(24), C(25), C(23), C(26) and C(27). A selection of bond distances and angles involving non-hydrogen atoms is given in Table 3. The geometry about the tin atom is that of a distorted octahedron. Although the Sn–N bond lengths show no significant differences, Sn-Cl(1), which lies in the mirror plane is *ca.* 0.01 Å longer than Sn–Cl(2). There are also angular distortions

Table 1 Summary of the crystal and refinement data for $[SnLCl_3]$

Formula	$C_{15}H_{22}BCl_3N_6Sn$
M	522.24
$F(000)$	520
Crystal system	monoclinic
Space group	$P2_1/m$
a/Å	8.148(1)
b/Å	14.208(2)
c/Å	9.225(1)
β/°	100.33(1)
U/Å^3	1050.6
T/°C	23 ± 1
Z	2
D_c/ g cm^{-3}	1.65
λ(Mo-Kα)/Å	0.710 73
μ/cm^{-1}	16.2
Crystal dimensions/mm	0.50 × 0.50 × 0.25
Scan rate/° min^{-1}	2–8
Scan type	θ–2θ
Scan width/°	$2.0 + (2\theta K_{\alpha 2} - 2\theta K_{\alpha 1})$
Maximum 2θ/°	50
No. reflections measured	2087 total, 1940 unique
Least-squares weights	$4F^2/[\sigma^2(I) + (pF^2)^2]$
$R = \Sigma(\|F_o\| - \|F_c\|)/\Sigma\|F_o\|$	0.022
$R' = [\Sigma w(\|F_o\| - \|F_c\|)^2/\Sigma w\|F_o\|^2]^{\frac{1}{2}}$	0.037
Maximum, minimum residual electron density/e Å^{-3}	0.40(6), −0.48(6)

Table 2 Positional parameters of the non-hydrogen atoms and their standard deviations for $[SnLCl_3]$

Atom	x	y	z
Sn	0.068 89(3)	0.250	0.300 80(2)
Cl(1)	0.316 4(1)	0.250	0.484 7(1)
Cl(2)	−0.058 8(1)	0.372 80(6)	0.416 07(8)
N(11)	0.180 0(3)	0.353 0(2)	0.169 0(2)
N(12)	0.163 6(2)	0.338 5(2)	0.018 8(2)
N(21)	−0.140 1(4)	0.250	0.113 2(3)
N(22)	−0.106 8(4)	0.250	−0.029 0(3)
C(13)	0.229 2(3)	0.412 9(2)	−0.041 2(3)
C(14)	0.289 3(4)	0.474 6(2)	0.069 2(4)
C(15)	0.257 2(4)	0.436 7(2)	0.198 9(3)
C(16)	0.233 9(5)	0.419 5(3)	−0.203 0(4)
C(17)	0.304 4(5)	0.476 7(3)	0.350 5(4)
C(23)	−0.250 0(5)	0.250	−0.126 0(4)
C(24)	−0.379 6(5)	0.250	−0.047 2(5)
C(25)	−0.310 0(5)	0.250	0.099 8(5)
C(26)	−0.255 0(6)	0.250	−0.288 4(5)
C(27)	−0.397 0(5)	0.250	0.228 8(6)
B	0.076 1(5)	0.250	−0.053 6(4)

compared with a regular octahedral structure, in that the bond angles involving the co-ordinated nitrogen atoms are all < 90°, whilst those involving chlorine are > 90°. The bond distances and angles involving equivalent types of atoms within the ligand L show no significant differences. The dimensions are comparable with those in other structures we have studied which involve this ligand.

The structure of $[MoO(L)Cl_2]$ has been determined[17] as the chlorobenzene solvate. The compound also crystallises in the monoclinic space group $P2_1/m$ with C_s symmetry imposed on the molecule by the space group. The Cl and O atoms were found to be randomly disordered over the three possible sites, and the apparent Mo–Cl(O) distances ranged from 2.27 to 2.17 Å. The apparent Cl(O)–Mo–Cl angles ranged from 96 to 98°.

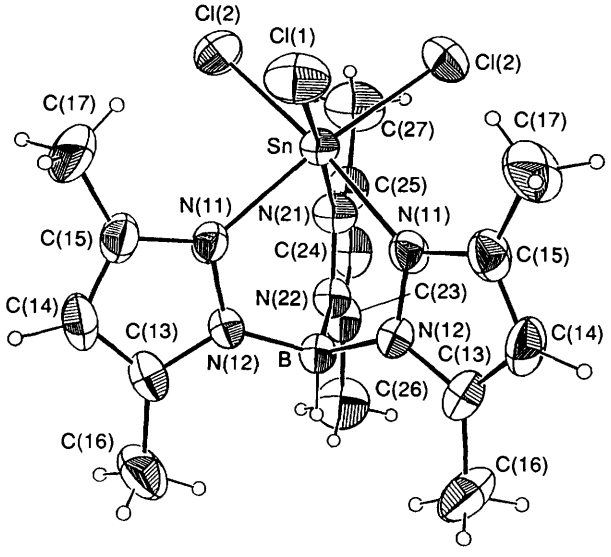

Fig. 1 Molecular structure and atomic numbering of $[SnLCl_3]$

Table 3 Selected bond distances (Å) and angles (°) involving non-hydrogen atoms for $[SnLCl_3]$

Sn–Cl(1)	2.3912(9)	N(22)–C(23)	1.337(4)
Sn–Cl(2)	2.3778(6)	N(22)–B	1.546(4)
Sn–N(11)	2.198(2)	C(13)–C(14)	1.366(4)
Sn–N(21)	2.199(3)	C(13)–C(16)	1.503(3)
N(11)–N(12)	1.384(2)	C(14)–C(15)	1.379(4)
N(11)–C(15)	1.350(3)	C(15)–C(17)	1.495(4)
N(12)–C(13)	1.347(3)	C(23)–C(24)	1.385(5)
N(12)–B	1.538(2)	C(23)–C(26)	1.492(5)
N(21)–N(22)	1.387(3)	C(24)–C(25)	1.373(5)
N(21)–C(25)	1.368(4)	C(25)–C(27)	1.490(5)
Cl(1)–Sn–Cl(2)	93.64(2)	N(21)–N(22)–B	119.7(2)
Cl(1)–Sn–N(11)	90.79(5)	C(23)–N(22)–B	130.6(3)
Cl(1)–Sn–N(21)	173.55(7)	N(12)–C(13)–C(14)	108.2(2)
Cl(2)–Sn–Cl(2)	94.40(3)	N(12)–C(13)–C(16)	122.6(2)
Cl(2)–Sn–N(11)	90.90(5)	C(14)–C(13)–C(16)	129.2(2)
Cl(2)–Sn–N(11)	172.86(5)	C(13)–C(14)–C(15)	107.4(2)
Cl(2)–Sn–N(21)	90.73(5)	N(11)–C(15)–C(14)	108.7(2)
N(11)–Sn–N(11)	83.44(9)	N(11)–C(15)–C(17)	124.0(2)
N(11)–Sn–N(21)	84.40(7)	C(14)–C(15)–C(17)	127.3(2)
Sn–N(11)–N(12)	118.7(1)	N(22)–C(23)–C(24)	107.8(3)
Sn–N(11)–C(15)	134.1(2)	N(22)–C(23)–C(26)	122.4(3)
N(12)–N(11)–C(15)	107.0(2)	C(24)–C(23)–C(26)	129.8(3)
N(11)–N(12)–C(13)	108.7(2)	C(23)–C(24)–C(25)	107.4(3)
N(11)–N(12)–B	120.7(2)	N(21)–C(25)–C(24)	108.7(3)
C(13)–N(12)–B	130.6(2)	N(21)–C(25)–C(27)	123.2(3)
Sn–N(21)–N(22)	119.3(2)	C(24)–C(25)–C(27)	128.2(3)
Sn–N(21)–C(25)	134.4(2)	N(12)–B–N(12)	109.7(2)
N(22)–N(21)–C(25)	106.4(3)	N(12)–B–N(22)	108.7(2)
N(21)–N(22)–C(23)	109.7(3)		

Numbers in parentheses are estimated standard deviations in the least significant digits.

EPR Spectra.—The disorder of the Cl and O atom sites observed in the structure of $[MoO(L)Cl_2]$[17] and the similarity between the molecular geometry of $[MoO(L)Cl_2]$ and that of $[SnLCl_3]$ suggest that the $[MoE(L)X_2]$ species may occupy all three SnCl sites when diluted into a crystal of $[SnLCl_3]$. If MoE occupies the SnCl(1) site (hereafter called site 1) we would expect EPR signals from only one type of magnetic molecule in all planes in the crystal. If MoE occupies the SnCl(2) and its mirror-related site SnCl(2A) (hereafter called sites 2 and 2A, respectively) we would expect to see signals from one type of magnetic site in the crystal *ac* plane, but from two magnetic sites in the other two crystal planes.

$[SnLCl_3\{MoO\}]$. The spectra in the three orthogonalised crystallographic planes were consistent with MoO occupying the three possible SnCl sites. No resolution of the separate ^{95}Mo and ^{97}Mo signals was found, and consequently only the mean values of the principal hyperfine tensors of $^{95,97}Mo$ are reported. This applies to each of the compounds in the present study. Although there was overlapping of spectra at some orientations, signals due to molecules in each site were identified and analysed. In principle the molecular g and A tensors for site 1 can be determined from measurements in the *ac* plane and parallel to the *b* axis. Except for our inability to identify clearly the metal hyperfine splitting for this site parallel to the *b* axis, this was achieved. The metal hyperfine value parallel to *b* was obtained from the least-squares-fitted curve for K^2g^2 in the a^*b plane. The spectra for molecules in sites 2 were treated by the methods of Schonland,[15] and Lund and Vånngard.[16] This treatment gives two alternative sets of values for the g^2 and K^2g^2 tensors, only one of which is correct. The reasons for making a selection between the alternatives are discussed for each individual system. The results of these analyses are summarised in Table 4 for site 1, and in Table 5 for sites 2 and 2A. There is a satisfactory degree of agreement between the values of the principal tensor elements, and between their relative orientations, obtained from site 1 and from sites 2. The coincidence of g_{22} and A_{22} for site 1 is crystallographically required because the diluent molecules occupy sites of mirror symmetry. The small angle of non-coincidence between these two tensor elements in sites 2 is

Table 4 Principal g and $A(^{95,97}Mo)$ values and their direction cosines with respect to the a^*bc axes for $[SnLCl_3\{MoO\}]$ in site 1

(*a*) Principal values and their direction cosines

	Direction cosine with respect to		
Value	a^*	b	c
$g_{11} = 1.931$	−0.8765	0.0000	0.4815
$g_{22} = 1.939$	0.0000	−1.0000	0.0000
$g_{33} = 1.969$	0.4815	0.0000	0.8765
$\langle g \rangle = 1.946$			
$g_{iso}^* = 1.947$			
$10^4\ A/cm^{-1}$			
$A_{11} = 33.8$	−0.4554	0.0000	0.8903
$A_{22} = 33.4$	0.0000	−1.0000	0.0000
$A_{33} = 71.6$	0.8903	0.0000	0.4554
$\langle A \rangle = 46.3$			
$A_{iso}^* = 46.0$			

(*b*) Intertensor angles (°)

	A_{11}	A_{22}	A_{33}
g_{11}	34.1	90.0	124.1
g_{22}	90.0	0.00	90.0
g_{33}	55.9	90.0	34.1

Estimated errors: g, ±0.001; A, ±0.5 × 10^{-4} cm^{-1}.

* Obtained from a fluid-solution spectrum in toluene.

Table 5 Principal g and $A(^{95,97}Mo)$ values and their direction cosines with respect to the a^*bc axes for $[SnLCl_3\{MoO\}]$ in site 2[a]

(*a*) Principal values and their direction cosines

	Direction cosine with respect to		
Value	a^*	b	c
$g_{11} = 1.932$	−0.4431	−0.7717	−0.4562
$g_{22} = 1.939$	0.8567	−0.5144	0.0382
$g_{33} = 1.967$	−0.2641	−0.3739	0.8891
$\langle g \rangle = 1.946$			
g_{iso}[b] $= 1.947$			
$10^4\ A/cm^{-1}$			
$A_{11} = 34.0$	−0.1540	−0.3956	−0.9054
$A_{22} = 32.1$	0.8835	−0.4654	0.0531
$A_{33} = 72.3$	−0.4424	−0.7918	0.4212
$\langle A \rangle = 46.1$			
A_{iso}[b] $= 46.0$			

(*b*) Intertensor angles (°)

	A_{11}	A_{22}	A_{33}
g_{11}	38.1	93.2	52.1
g_{22}	87.9	3.3	87.5
g_{33}	128.1	90.7	38.1

The Euler angles corresponding to these intertensor angles are: $\alpha = 94.1, \chi = 38.1, \gamma = 119.2°$.
Estimated errors: g, ±0.001; A, ±0.5 × 10^{-4} cm^{-1}.

[a] There is only one set of values since the other alternative gave a negative K^2g^2 element and was therefore rejected. [b] Obtained from a fluid-solution spectrum in toluene.

Table 6 Angles (°) between the EPR tensors and the Sn–X directions in $[SnLCl_3\{MoO\}]$, site 1

	X = Cl(1) (MoO)	Cl(2)	Cl(2A)	N(11)	N(11A)	N(21)
Choice 1						
g_{11}	117.3	50.9	50.9	131.1	131.1	69.2
g_{22}	90.0	137.2	42.8	131.7	48.3	90.0
g_{33}	27.3	75.3	75.3	110.8	110.8	159.2
A_{11}	83.2	48.4	48.4	137.9	137.9	103.3
A_{22}	90.0	137.2	42.8	131.7	48.2	90.0
A_{33}	6.8	98.3	98.3	85.7	85.7	166.7
Choice 2						
g_{11}	5.2	97.1	97.1	86.9	86.9	168.4
g_{22}	90.0	42.8	137.2	48.3	131.7	90.0
g_{33}	84.8	48.1	48.1	138.1	138.1	101.6
A_{11}	29.0	74.2	74.2	111.9	111.9	157.5
A_{22}	90.0	42.8	137.2	48.3	131.7	90.0
A_{33}	119.0	51.5	51.5	130.2	130.2	67.5

consistent with the structure of the host, since there is now no requirement for the diluent molecule to have mirror symmetry. Apart from A_{22}, which was the most difficult parameter to determine from the frozen-solution spectra, there is good agreement between the other parameters determined from the single-crystal study and the simulation of the frozen-solution spectra.[1]

Relationship between EPR tensors and molecular structure. Each alternative for the g^2 and K^2g^2 tensors is, *a priori*, associated with four choices of the direction cosines of the principal values of these two tensors with respect to the crystal axes. These choices arise from not knowing the positive and negative senses of the measurement axes with respect to the crystallographic axes. Using the direction cosines from Table 4, the fractional coordinates from Table 2 and the possible assignments of the measuring axes, the orientations of the g and A tensors for site 1 have been related to the molecular geometry. Owing to the crystallography there are only two distinct choices. These are summarised in Table 6 and Fig. 2. Choice 1 has the largest A value (A_{33}) within 7° of SnCl(1)-(MoO) with g_{33} *ca.* 27° from this direction. This places g_{33} close to a pseudo-three-fold axis through the three pyrazole nitrogen atoms. The orientations of the two smaller A values bisect the Cl(2)–Sn–Cl(2A) and Cl(2)–Sn–N(11A) angles in positions analogous to those found for the 'in-plane' values in high-symmetry systems. Choice 2 from this treatment places the smallest g value (g_{11}) 5.2° from SnCl(1)(MoO) with A_{11} 29.0° from this direction. In this choice it is the orientations of the other g values which approximately bisect the 'in-plane' ligand directions. The same procedures were used for the data from sites 2. The patterns of orientations of the principal axes with respect to the molecular framework are similar, with only small differences in angular displacements. The results are summarised in Table 7. A selection between the two choices of assignment of the tensors to the molecular geometry has to be made. We, and others, have previously[2,18–20] used the criterion that the A tensor will be close to metal-ligand bond

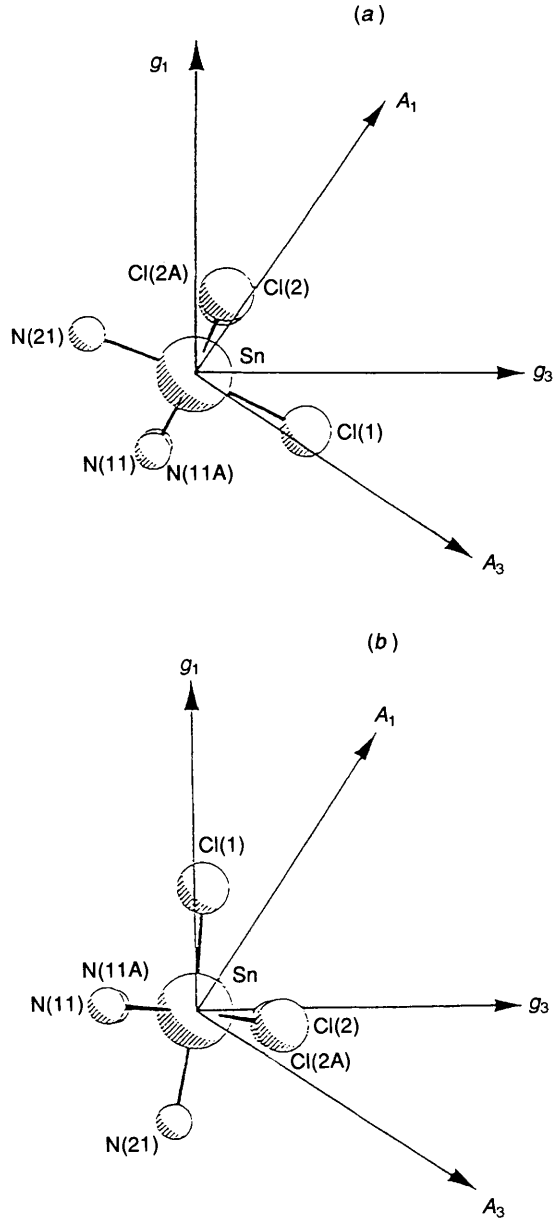

Fig. 2 Orientation of the principal g and A values with respect to the molecular structure of $[SnLCl_3\{MoO\}]$. The view is down the $g_{22}(A_{22})$ direction which is perpendicular to the mirror plane (the plane of the page) of the molecule. The directions of the principal axes of g_1, g_3, A_1, A_3, shown in the diagram, are in the mirror plane. (*a*) Choice 1, (*b*) choice 2

directions or pseudo-symmetry axes, and that with the largest value is close to Mo-E (as occurs in high-symmetry systems). On this basis choice 1 is our preferred assignment.

[$SnLCl_3${MoS}]. Apart from the resonances being at different magnetic fields, the spectra for this system behaved in a similar manner to those of the corresponding oxo compound. In addition to the sulfido species, the EPR spectra indicated that the crystals contained *ca.* 10% of the oxo compound. However, the signals for this impurity were usually sufficiently separate from those of the sulfido species for them to be identified. There were a few orientations where the signal from the oxo species interfered with the measurement of the metal hyperfine spectrum of the sulfido derivative. The analysis of the spectra followed that for the oxo species above, except for the determination of the metal hyperfine value parallel to the *b* axis. In this case we could not reliably identify sufficient hyperfine data for site 1 molecules in the a^*b plane to allow a satisfactory least-squares fit. Instead A_{bb} was calculated from A_{max} and A_{min} in the a^*c plane, together with A_{iso} from a fluid-solution spectrum. The results of the analyses of the spectra for site 1 are in Table 8 and those for sites 2 are in Table 9. Alternative II in Table 9 was preferred on the basis that it gave (*i*) better simulations of the powder spectra of the diluted material at both X- and Q-band frequencies, and (*ii*) closer agreement with the results from site 1. As in the case of the oxo species, the molecules occupying sites 2 give EPR parameters which only approximate to those expected for C_s point symmetry.

There is good agreement between the angle of non-coincidence of the monoclinic *g* and *A* tensors determined from both the single-crystal study and from simulation of the frozen-solution spectra.[2] Similarly the principal values of the *A*-tensor elements in the mirror plane are in reasonable agreement from the two methods but, as for the oxo-derivative, there is poor agreement between the values of A_{22}. The relative values of the principal *g*-tensor elements are similar for the two methods. However, the values of corresponding g_{ii} are significantly different from the single-crystal study compared to those from

Table 7 Angles (°) between the EPR tensors and the Sn–X directions in [$SnLCl_3${MoO}], site 2

Choice 1

X =	Cl(1)	Cl(2)	Cl(2A)(MoO)	N(11)	N(11A)	N(21)
g_{11}	128.5	128.0	58.9	114.0	51.7	50.7
g_{22}	42.9	136.6	88.4	91.1	48.3	132.6
g_{33}	73.9	72.1	31.2	155.9	114.5	112.0
A_{11}	129.3	134.3	96.9	76.0	39.8	45.3
A_{22}	40.3	133.9	90.6	89.1	50.6	135.0
A_{33}	97.6	99.7	6.9	166.0	85.2	86.3

Choice 2

X =	Cl(1)	Cl(2)(MoO)	Cl(2A)	N(11)	N(11A)	N(21)
g_{11}	96.5	4.6	97.8	87.2	168.3	87.6
g_{22}	46.4	90.7	140.0	44.5	88.4	128.9
g_{33}	135.7	94.5	128.9	45.6	78.4	39.0
A_{11}	67.8	33.6	75.4	111.5	153.3	118.0
A_{22}	45.3	93.8	138.6	45.5	85.3	129.7
A_{33}	127.0	56.8	127.7	52.3	116.3	52.4

Table 8 Principal *g* and $A(^{95,97}Mo)$ values and their direction cosines with respect to the a^*bc axes for [$SnLCl_3${MoS}] in site 1

(*a*) Principal values and their direction cosines

	Direction cosine with respect to		
Value	a^*	*b*	*c*
g_{11} = 1.900	0.8534	0.0000	−0.5213
g_{22} = 1.911	0.0000	1.0000	0.0000
g_{33} = 1.958	0.5213	0.0000	0.8534
$\langle g \rangle$ = 1.923			
g_{iso}* = 1.928			
10^4 *A*/cm^{-1}			
A_{11} = 37.0	0.4686	0.0000	−0.8834
A_{22} = 33.7	0.0000	1.0000	0.0000
A_{33} = 69.7	0.8834	0.0000	0.4686
$\langle A \rangle$ = 46.8			
A_{iso}* = 46.8			

(*b*) Intertensor angles (°)

	A_{11}	A_{22}	A_{33}
g_{11}	30.7	90.0	59.3
g_{22}	90.0	0.00	90.0
g_{33}	120.7	90.0	30.7

Estimated errors: *g*, ±0.001; *A*, ±0.5 × 10^{-4} cm^{-1}.

* Obtained from a fluid-solution spectrum in toluene.

Table 9 Principal *g* and $A(^{95,97}Mo)$ values and their direction cosines with respect to the a^*bc axes for [$SnLCl_3${MoS}] in site 2

Alternative I

(*a*) Principal values and their direction cosines

	Direction cosine with respect to		
Value	a^*	*b*	*c*
g_{11} = 1.904	0.4681	−0.7372	0.4873
g_{22} = 1.917	0.8446	0.5354	−0.0013
g_{33} = 1.954	−0.2599	0.4121	0.8733
$\langle g \rangle$ = 1.925			
g_{iso}* = 1.928			
10^4 *A*/cm^{-1}			
A_{11} = 10.8	0.6419	−0.4909	0.5891
A_{22} = 68.0	0.3493	0.8711	0.3452
A_{33} = 52.4	0.6826	0.0158	−0.7306
$\langle A \rangle$ = 43.7			
A_{iso}* = 46.8			

(*b*) Intertensor angles (°)

	A_{11}	A_{22}	A_{33}
g_{11}	18.3	108.1	92.8
g_{22}	73.8	40.5	54.1
g_{33}	81.7	55.3	144.0

The Euler angles corresponding to these intertensor angles are: α = 4.7, χ = 36.0, γ = 14.3°.

Alternative II

(*a*) Principal values and their direction cosines

	Direction cosine with respect to		
Value	a^*	*b*	*c*
g_{11} = 1.905	−0.4227	−0.7581	−0.4966
g_{22} = 1.916	0.8643	−0.5020	0.0306
g_{33} = 1.954	−0.2724	−0.4163	0.8675
$\langle g \rangle$ = 1.925			
g_{iso}* = 1.928			
10^4 *A*/cm^{-1}			
A_{11} = 36.2	−0.2169	−0.3912	−0.8944
A_{22} = 33.4	0.8711	−0.4911	0.0036
A_{33} = 71.2	−0.4407	−0.7783	0.4473
$\langle A \rangle$ = 46.9			
A_{iso}* = 46.8			

(*b*) Intertensor angles (°)

	A_{11}	A_{22}	A_{33}
g_{11}	33.7	89.9	56.3
g_{22}	91.1	1.7	88.7
g_{33}	123.6	91.7	33.7

The Euler angles corresponding to these intertensor angles are: α = 92.4, χ = 33.7, γ = 266.9°.

Estimated errors: *g*, ±0.002; *A*, ±1.0 × 10^{-4} cm^{-1}.

* Obtained from a fluid-solution spectrum in toluene.

Table 10 Angles (°) between the EPR tensors and the Sn–X directions in $[SnLCl_3\{MoS\}]$, site 1

	X = Cl(1)(MoS)	Cl(2)	Cl(2A)	N(11)	N(11A)	N(21)
Choice 1						
g_{11}	65.4	129.9	129.9	47.7	47.7	108.2
g_{22}	90.0	42.8	137.2	48.3	131.7	90.0
g_{33}	24.6	77.0	77.0	108.9	108.9	161.8
A_{11}	96.0	131.8	131.8	42.0	42.0	77.5
A_{22}	90.0	42.8	137.2	48.3	131.7	90.0
A_{33}	6.0	97.7	97.7	86.3	86.3	167.5
Choice 2						
g_{11}	2.5	95.4	95.4	88.9	88.9	171.0
g_{22}	90.0	137.2	42.8	131.7	48.3	90.0
g_{33}	92.5	132.3	132.3	41.7	41.7	81.0
A_{11}	28.1	74.8	74.8	111.3	111.3	158.3
A_{22}	90.0	137.2	42.8	131.7	48.3	90.0
A_{33}	61.9	128.8	128.8	49.3	49.3	111.7

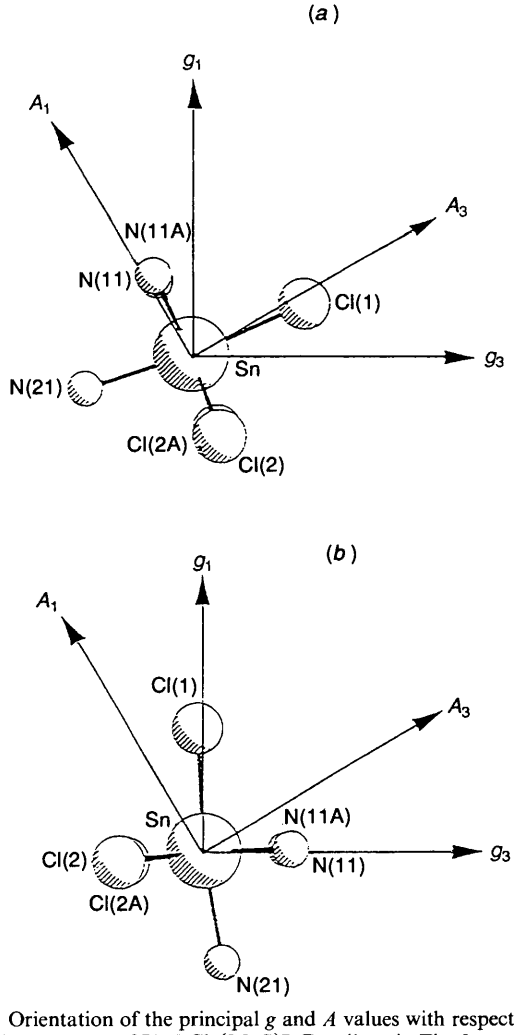

Fig. 3 Orientation of the principal g and A values with respect to the molecular structure of $[SnLCl_3\{MoS\}]$. Details as in Fig. 2.

the frozen-solution spectrum. The observation of similar principal A values between the crystal and frozen-solution studies, but significant differences between the principal g values from the two methods, is analogous to the findings of Nilges and Belford[20] for $[MoO(NCS)_5]^{2-}$. These authors found that the principal g values and their orientations were sensitive to the site environment, whilst the principal A values showed no such dependence.

Relationship between EPR tensors and the molecular structure.

Table 11 Angles (°) between the EPR tensors and the Sn–X directions in $[SnLCl_3\{MoS\}]$, site 2

Choice 1						
	X = Cl(1)	Cl(2)	Cl(2A)(MoS)	N(11)	N(11A)	N(21)
g_{11}	128.9	129.4	61.5	111.4	49.9	49.9
g_{22}	42.8	136.4	89.3	90.2	48.3	132.7
g_{33}	75.0	74.5	28.5	158.6	112.1	110.8
A_{11}	132.8	131.6	95.1	77.7	42.8	41.9
A_{22}	43.6	137.2	90.7	88.6	47.4	131.7
A_{33}	96.7	98.4	5.2	167.7	86.6	87.4
Choice 2						
	X = Cl(1)	Cl(2)(MoS)	Cl(2A)	N(11)	N(11A)	N(21)
g_{11}	94.2	2.2	96.5	88.7	170.8	90.0
g_{22}	45.6	91.1	139.2	45.3	88.0	129.7
g_{33}	135.3	91.9	130.1	44.7	81.0	39.7
A_{11}	71.4	31.7	74.0	112.8	155.3	114.5
A_{22}	43.9	90.9	137.5	47.0	88.4	131.4
A_{33}	128.0	58.3	128.1	51.7	114.6	51.3

The EPR data in Tables 8 and 9 were treated in the same way as those for the oxo derivative. The results for site 1 are summarised in Table 10 and Fig. 3, and they are similar to those found for the oxo derivative. For choice 1 the largest A value (A_{33}) is 6.0° from SnCl(1)(MoS) with g_{33} 24.6° away. For the reasons cited above for the oxo-derivative, this is the preferred choice. The other two A tensors are between the 'in-plane' ligands. For choice 2 the smallest g value (g_{11}) is 2.5° from SnCl(1)(MoS) with A_{11} 28.1° away from this direction. As for the oxo-derivative, the orientations of the other g values are now approximately bisecting the 'in-plane' ligands. With only small differences in angular displacements, the results for sites 2 are similar to those for site 1. The results are summarised in Table 11.

$[SnLCl_3\{MoO(NCS)_2\}]$. The single-crystal EPR spectra in the *ab*, *bc**, and *ac** planes were compatible with the molybdenum compound occupying only sites 2. The spectra were analysed using the Schonland method to give the two numerical alternatives in Table 12. The simulation of the powder spectra at both X- and Q-band frequencies showed alternative I to be the most appropriate. As we found for the two other compounds studied, the EPR symmetry of the molecules which occupy sites 2 is strictly triclinic. In the present case the angle of non-coincidence between g_{22} and A_{22} is small (2.6°). The presence of such a small angle of non-coincidence would not be detected from the powder spectra, since we found that simulations assuming monoclinic symmetry (α_t = 28°) were indistinguishable from those above. In addition to the parameters giving a good simulation of the powder spectra of $[SnLCl_3\{MoO(NCS)_2\}]$, they are also in very good agreement with those required to simulate[1] the frozen-solution spectra of $[MoO(L)(NCS)_2]$ in toluene.

Relationship between EPR tensors and molecular structure. The mirror symmetry of the host reduces the number of ways of relating the EPR tensors of this system to the molecular geometry to just two choices. The angles between the principal directions of the tensors and the co-ordination sphere of the host are given in Table 13 and in Fig. 4. Choice 1 places the largest A value (A_{11}) *ca.* 6° from SnCl(2)(MoO) and its associated g value (g_{11}) *ca.* 36° from this direction. The orientations of the other A tensors are between the 'in-plane' N(11)–Sn–N(21) (A_{33}) and Cl(1)–Sn–N(11) (A_{22}) angles. In addition this choice places the nearly coincident g and A values (g_{22} and A_{22}) close to the perpendicular of the pseudo-mirror plane for site 2 in the crystal. As for the case of site 1, choice 1, for $[MoO(L)Cl_2]$ the orientation of the largest g value (g_{33}) is close to the pseudo-three-fold axis defined by the co-ordinated nitrogen atoms of L. For choice 2, g_{11} was *ca.* 17° from SnCl(2A)(MoO) whilst A_{11} is *ca.* 46° from this direction. However, the nearly coincident g and A values are not as

Table 12 Principal g and $A(^{95,97}Mo)$ values and their direction cosines with respect to the abc^* axes for $[SnLCl_3\{MoO(NCS)_2\}]$ in site 2

Alternative I

(*a*) Principal values and their direction cosines

	Direction cosine with respect to		
Value	*a*	*b*	*c**
$g_{11} = 1.931$	−0.5505	0.8182	−0.1657
$g_{22} = 1.945$	0.8059	0.5727	0.1505
$g_{33} = 1.954$	0.2180	−0.0507	−0.9746
$\langle g \rangle = 1.943$			
$g_{iso}^* = 1.943$			
$10^4\ A/cm^{-1}$			
$A_{11} = 68.5$	0.5497	−0.7598	−0.3471
$A_{22} = 32.0$	0.8311	0.5393	0.1357
$A_{33} = 30.5$	−0.0841	0.3631	−0.9280
$\langle A \rangle = 43.7$			
$A_{iso}^* = 42.9$			

(*b*) Intertensor angles (°)

	A_{11}	A_{22}	A_{33}
g_{11}	150.1	92.2	60.2
g_{22}	92.5	2.6	90.0
g_{33}	60.2	88.8	29.8

The Euler angles corresponding to these intertensor angles are: $\alpha = 270.1$, $\chi = 150.2$, $\gamma = 87.5°$.

Alternative II

(*a*) Principal values and their direction cosines

	Direction cosine with respect to		
Value	*a*	*b*	*c**
$g_{11} = 1.931$	0.5422	−0.8402	−0.0138
$g_{22} = 1.944$	−0.7760	−0.4943	−0.3918
$g_{33} = 1.954$	−0.3223	−0.2231	0.9200
$\langle g \rangle = 1.943$			
$g_{iso}^* = 1.943$			
$10^4\ A/cm^{-1}$			
$A_{11} = 65.6$	0.5356	−0.8301	0.1548
$A_{22} = 3.4$	0.5746	0.4926	0.6535
$A_{33} = 48.2$	−0.6188	−0.2611	0.7409
$\langle A \rangle = 39.1$			
$A_{iso}^* = 42.9$			

(*b*) Intertensor angles (°)

	A_{11}	A_{22}	A_{33}
g_{11}	9.7	96.4	97.3
g_{22}	93.8	161.0	71.4
g_{33}	81.1	72.2	20.1

The Euler angles corresponding to these intertensor angles are: $\alpha = 21.6$, $\chi = 159.9$, $\gamma = 26.9°$.
Estimated errors: g, ±0.001; A, ±0.5 × 10^{-4} cm^{-1}.

* Obtained from a fluid-solution spectrum in toluene.

Table 13 Angles (°) between the EPR tensors and the Sn–X directions in $[SnLCl_3\{MoO(NCS)_2\}]$, site 2

Choice 1

X = Cl(1)	Cl(2)(MoO)	Cl(2A)	N(11)	N(11A)	N(21)
g_{11} 120.7	35.7	112.8	69.3	137.4	61.5
g_{22} 47.0	86.0	140.5	44.7	92.9	128.8
g_{33} 121.6	125.4	120.3	52.6	47.5	51.9
A_{11} 98.7	5.8	96.9	87.9	167.3	85.5
A_{22} 46.4	88.6	140.0	44.8	90.5	129.1
A_{33} 135.1	95.6	129.1	45.3	77.3	39.5

Choice 2

X = Cl(1)	Cl(2)	Cl(2A)(MoO)	N(11)	N(11A)	N(21)
g_{11} 106.2	104.0	16.6	156.3	80.0	77.3
g_{22} 61.8	154.6	93.6	83.5	29.0	113.2
g_{33} 33.2	69.3	73.8	112.7	116.9	153.2
A_{11} 129.5	115.2	46.4	126.7	65.6	51.9
A_{22} 60.0	152.3	95.4	82.0	31.0	114.9
A_{33} 54.0	79.3	44.1	142.1	107.8	131.7

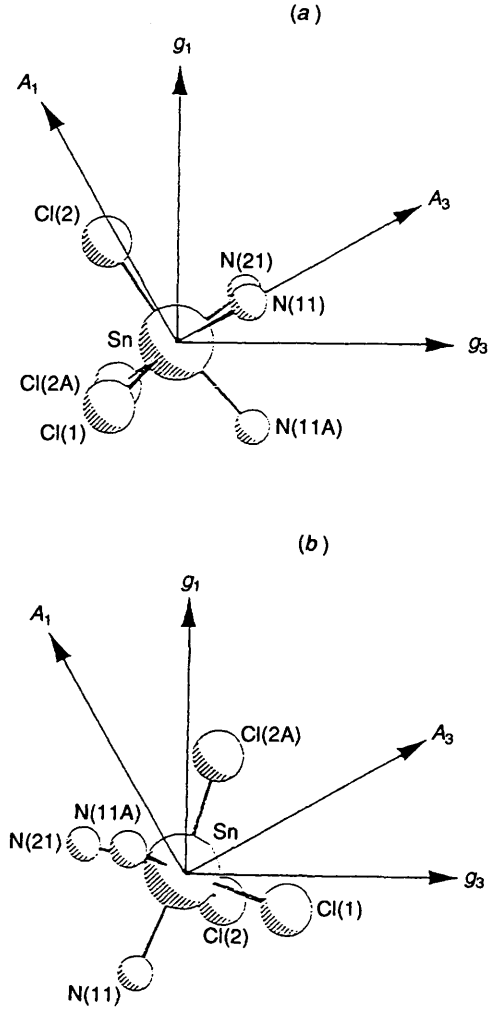

Fig. 4 Orientation of the principal g and A values with respect to the molecular structure of $[SnLCl_3\{MoO(NCS)_2\}]$. The view is down the $g_{22}(A_{22})$ direction with the directions of the other principal values in the plane of the paper. The text describes the orientations of the principal values with respect to the atomic framework. (*a*) Choice 1, (*b*) choice 2

close to the pseudo-mirror plane for the molecule as they were in choice 1, which suggests that choice 2 is probably less likely. Based on the criteria cited for the $[MoO(L)Cl_2]$ case, and the closer approximation of g_{22} and A_{22} to the normal to the pseudo-mirror plane, choice 1 is the preferred assignment. This assignment is analogous to that[20] for $\{MoO\}^{3+}$ in $[AsPh_4][NbO(NCS)_5]$, in which there is $\{MoON_5\}$ co-ordination. In this system, where the site symmetry at the molybdenum is also low (less than C_{2v}), the orientations of the A tensors are close to the pseudo-symmetry axes with the largest within *ca.* 3° of the MoO direction. The smallest g value is rotated 14° from this direction.

The relationship between the g *and* A *tensors and the electronic structures*. The magnitudes of the g- and A-tensor elements depend upon the orbital wavefunctions and on the relative energies of the ground and excited states.[21] The detailed form of the wavefunctions depends upon the point symmetry of the compound. For C_s point symmetry with z parallel to Mo–E

and y perpendicular to the mirror plane, the permitted d-orbital mixings are given in equations (1)–(5) where α, β, γ, δ, and ε are

$$\varphi_1 = \alpha(a_1 d_{x^2-y^2} + b_1 d_{xz} + c_1 d_{z^2}) \quad |a_1| > |b_1, c_1| \quad (1)$$

$$\varphi_2 = \beta(a_2 d_{x^2-y^2} + b_2 d_{xz} + c_2 d_{z^2}) \quad |b_2| > |a_2, c_2| \quad (2)$$

$$\varphi_3 = \gamma(e_3 d_{xy} + f_3 d_{yz}) \quad |e_3| > |f_3| \quad (3)$$

$$\varphi_4 = \delta(e_4 d_{xy} + f_4 d_{yz}) \quad |f_4| > |e_4| \quad (4)$$

$$\varphi_5 = \varepsilon(a_5 d_{x^2-y^2} + b_5 d_{xz} + c_5 d_{z^2}) \quad |c_5| > |a_5, b_5| \quad (5)$$

metal molecular orbital coefficients. Within this metal-based d-orbital mixing scheme, the relationships between the d-orbital mixing and the g- and A-tensor elements are complicated[2,22] and have a non-linear dependence on the mixing coefficients. In addition the g-tensor elements depend upon the energies of the excited states. The expressions for the off-diagonal tensor elements are (6) and (7) where Δ_i is the energy separation

$$g_{xz} = g_{zx} = [2\xi(\alpha\gamma)^2(b_1 e_3 + a_1 f_3 + 3^{\frac{1}{2}} c_1 f_3) \times (2a_1 e_3 + b_1 f_3)/\Delta_3] + [2\xi(\alpha\delta)^2(b_1 e_4 + a_1 f_4 + 3^{\frac{1}{2}} c_1 f_4) \times (2a_1 e_4 + b_1 f_4)/\Delta_4] \quad (6)$$

$$A_{xz} = A_{zx} = P\{[2\alpha^2(3a_1 b_1 + 3^{\frac{1}{2}} b_1 c_1)/7] + g_{xz}\} \quad (7)$$

between φ_1 and φ_i and ξ is the single-electron spin-orbit coupling constant of the metal.

For the compounds in the present study only one transition energy to these excited states can be found experimentally because of the presence of intense low-energy charge-transfer bands. In addition there may also be contributions, particularly to the g-tensor elements, from charge-transfer states[1,2,21] and from spin–orbit coupling on the ligands.[21] These factors mean that it is not possible to determine the d-orbital mixing directly from the EPR data. We have attempted to overcome this by calculating the EPR parameters using both an angular-overlap model[22–26] and Fenske–Hall[2,27,28] molecular-orbital calculations. Although we have found the angular-overlap model satisfactory for similar oxovanadium(IV) compounds,[14] it was unsatisfactory for the present compounds. This is because in the vanadium systems we were able to determine the energies of the excited states experimentally, and to use them as one criterion for an acceptable fit. In addition, charge-transfer states are likely to make a smaller contribution to the g tensor due to the smaller value of ξ for vanadium. Similarly the Fenske–Hall calculations were also unsatisfactory, since the calculated d-orbital mixings were not compatible with the large value of α_1, and the energy separations to the excited states could not be calculated with sufficient accuracy. In both models we found it impossible to calculate correctly and simultaneously the values of all the g-tensor elements, even when ligand spin–orbit coupling was included in the Fenske–Hall calculations.

In view of the above difficulties, we confine the discussion to a qualitative treatment. The A-tensor elements are determined mainly by the composition of the ground state. The relatively small variation in the principal A values between the compounds studied suggests that this composition is not very different for the three compounds. This is compatible with the ground state consisting mainly of the essentially non-bonding $d_{x^2-y^2}$ orbital. If we assume that c_1 is zero and $P = -50 \times 10^{-4}$ cm^{-1}, the experimental data for [MoO(L)Cl$_2$] lead to values of a_1 ranging from 0.9960 to 0.9945 for $\alpha^2 = 1.0$ and 0.8, respectively. These values of a_1 are similar to those calculated *via* the Fenske–Hall method[2] for the ground-state orbital of the idealised species *fac*-[MoOCl$_2$(NH$_3$)$_3$]$^+$. Such a description, which is consistent with the observed metal hyperfine tensor, implies dominance of the terminal oxo (or sulfido) group leading to near-axial electronic symmetry in the ground state of these geometrically low-symmetry systems. On the other hand the g-tensor elements depend upon the composition of all of the states as well as on the energies of the excited states. Since there appears to be no extensive mixing in the ground state, the large angle of twist in these compounds must be due to considerable d-orbital mixing in the excited state orbitals φ_3 and φ_4. In C_s point symmetry the twist of the principal axes of the g tensor away from those of the A tensor depends upon the value of g_{xz}, which in turn depends upon the energies of, and d-orbital mixing in, the orbitals φ_3 and φ_4. Based on the assumption that g_{xx} and g_{zz} are orthogonal to the planes of φ_3 and φ_4, the mixing coefficients in φ_3 and φ_4 have previously[19] been related to the angle of twist, α_t, with $e_3 = \cos\alpha_t$, $f_3 = \sin\alpha_t$, $e_4 = \sin\alpha_t$, and $f_4 = -\cos\alpha_t$. This assumption cannot be generally correct, for the following reasons. (*i*) It is the value of g_{xz} which determines the rotation of the principal g values from the chosen axis system and also from the principal A values. The expression for g_{xz} derived from a simple d-orbital mixing approach[2,29] shows a direct proportionality to ξ, the spin–orbit coupling constant of the metal. Thus for example if there is the same degree of d-orbital mixing and the same energy separations for a vanadium(IV) and a molybdenum(V) compound, the angle of rotation would be larger for the latter because of its larger spin–orbit coupling constant. (*ii*) Similarly there is an inverse relationship of g_{xz} to ΔE. The molybdenum hyperfine values for [MoO(L)Cl$_2$] and [MoS(L)Cl$_2$] are similar, implying that their ground states are also of a similar composition. Since at least one d–d transition which would be expected to contribute to the calculation of g_{xz} is at lower energy for the sulfido compound,[2] we would expect α_t to be larger for this derivative compared to the oxo compound. The direct determination of α_t from site 1 for each of these compounds shows the opposite to be true. (*iii*) The small angles of twist observed experimentally for [VO(L)(S$_2$CNR$_2$)] would imply little mixing of the d orbitals in φ_3 and φ_4. However *both* the d–d spectra *and* the EPR parameters are fairly well modelled by the angular overlap model, *but only* when the model produces values of e_i and f_i which, based on the above assumptions, calculate α_t to be greater than the values observed.

For our preferred choices of the orientations of the principal axes of the g and A tensors, g_{33} is close to the pseudo-three-fold axis of the molecule in each case. Since the values and orientations of the principal components of the g tensor depend upon the excited states, this suggests qualitatively that a description of these excited states may be based upon a trigonally distorted octahedral model. Since the excited states, which are closest to the ground state and which contribute to the g tensor, involve π bonding to the terminal oxo-group, transfer of the unpaired electron into these orbitals would weaken this π bonding, thus reducing the ligand-field effect of the oxo-group. Such a weakening, with the concomitant strengthening of the ligand field from the *trans*-nitrogen atom, may allow the facially co-ordinated L ligand to have an increased contribution to the overall ligand field compared to that in the ground state.

When using the EPR parameters of low symmetry, d^1, oxo(sulfido)metal systems the ground state can be described with some confidence from a detailed knowledge of the metal hyperfine tensor. However, a similar degree of confidence does not extend to the use of the g tensor. Since the inclusion of ligand spin–orbit coupling, *via* the Fenske–Hall calculations, leads to no improvement in the calculation of the EPR parameters, alternative effects must be considered in order to account for the values of the g tensor of the molybdenum compounds. The method of calculation used assumed that the composition and energies of the excited states can be derived directly from the ground-state description. It appears that, in the present low-symmetry systems, such an extrapolation from the ground state is inadequate. It is the mixing of the electronic excited states into the ground state *via* spin–orbit coupling that determines the g tensor (see above). Thus we may anticipate

that there may be both large differences between α_t for similar vanadium(IV) and molybdenum(V) compounds, and in the ability for the EPR parameters of the latter metal to be modelled adequately. Thus spectroscopic techniques which monitor excited states with relatively high resolution (*e.g.* single-crystal EPR, electronic absorption, resonance-Raman) may produce very different relationships between the electronic parameters and molecular geometries of compounds of these two transition-metal ions. We are currently investigating other mixed-ligand low-symmetry compounds of both the early and late d transition metals by EPR spectroscopy to determine these effects further.

Acknowledgements

We thank The Royal Society (D. C. for a research fellowship), the SERC (K. R. for a quota studentship), and the University of Manchester (D. R. E. for a postgraduate award) for financial support. J. H. E. also gratefully acknowledges partial support of this work by the U.S. National Institutes of Health.

References

1 D. Collison, F. E. Mabbs, J. H. Enemark and W. E. Cleland, jun., *Polyhedron*, 1986, **5**, 423.
2 C. G. Young, J. H. Enemark, D. Collison and F. E. Mabbs, *Inorg. Chem.*, 1987, **26**, 2925.
3 D. Collison, B. Gahan and F. E. Mabbs, *J. Chem. Soc., Dalton Trans.*, 1987, 111.
4 D. Collison, F. E. Mabbs and J. Temperley, *Spectrochim. Acta, Part A*, 1991, **47**, 691.
5 D. Collison, D. R. Eardley, F. E. Mabbs, K. Rigby and J. H. Enemark, *Polyhedron*, 1989, **8**, 1833.
6 W. E. Cleland, jun., K. M. Barnhart, K. Yamanouchi, D. Collison, F. E. Mabbs, R. B. Ortega and J. H. Enemark, *Inorg. Chem.*, 1987, **26**, 1017.
7 S. Trofimenko, *J. Am. Chem. Soc.*, 1967, **89**, 6288.
8 N. Walker and D. Stuart, *Acta Crystallogr., Sect. A*, 1983, **39**, 158.
9 D. T. Cromer and J. T. Waber, *International Tables for X-Ray Crystallography*, Kynoch Press, Birmingham, 1974, vol. 4, Table 2.2B.
10 J. A. Ibers and W. C. Hamilton, *Acta Crystallogr.*, 1964, **17**, 781.
11 D. T. Cromer, *International Tables for X-Ray Crystallography*, Kynoch Press, Birmingham, 1974, vol. 4, Table 2.3.1.
12 D. W. J. Cruickshank, *Acta Crystallogr.*, 1949, **2**, 154.
13 B. A. Frenz, The Enraf-Nonius CAD 4 SDP, A Real-time System for Concurrent X-Ray Data Collection and Crystal Structure Determination, in *Computing in Crystallography*, eds. H. Shenk, R. Olthof-Hazelkamp, H. van Konigsveld and G. C. Bassi, Delft University Press, Delft, 1978, pp. 64–71.
14 D. Collison, F. E. Mabbs, K. Rigby and W. E. Cleland, jun., *J. Chem. Soc., Faraday Trans.*, 1993, 3695.
15 D. S. Schonland, *Proc. Phys. Soc., London*, 1959, **73**, 788.
16 A. Lund and T. Vånngard, *J. Chem. Phys.*, 1965, **42**, 2979.
17 G. Ferguson, B. Kaitner, F. J. Lalor and G. Roberts, *J. Chem. Res.*, 1982, (*S*) 6.
18 C. D. Garner, P. Lambert, F. E. Mabbs and T. J. King, *J. Chem. Soc., Dalton Trans.*, 1977, 1191.
19 M. I. Scullane, R. D. Taylor, M. Minelli, J. T. Spence, K. Yamanouchi, J. H. Enemark and N. D. Chasteen, *Inorg. Chem.*, 1979, **18**, 3213.
20 M. J. Nilges and R. L. Belford, *J. Magn. Reson.*, 1979, **35**, 259.
21 F. E. Mabbs and D. Collison, *Electron Paramagnetic Resonance of d Transition Metal Compounds*, Elsevier, Amsterdam, 1992, ch. 9.
22 C. E. Schäffer, *Struct. Bonding (Berlin)*, 1968, **5**, 68; *Proc. R. Soc. London, Ser. A*, 1967, **297**, 96.
23 C. E. Schäffer and C. K. Jørgensen, *Mol. Phys.*, 1965, **9**, 401.
24 H. H. Schmidtke, *Z. Naturforsch., Teil A*, 1964, **19**, 1502.
25 C. K. Jørgensen, R. Pappalardo and H. H. Schmidtke, *J. Chem. Phys.*, 1963, **39**, 1422.
26 M. Gerloch and R. C. Slade, *Ligand Field Parameters*, Cambridge University Press, 1973, ch. 8.
27 M. B. Hall and R. F. Fenske, *Inorg. Chem.*, 1972, **11**, 768.
28 R. F. Fenske, *Pure Appl. Chem.*, 1971, **27**, 61.
29 F. E. Mabbs and D. Collison, *Electron Paramagnetic Resonance of d Transition Metal Compounds*, Elsevier, Amsterdam, 1992, pp. 386–389.

Received 29*th September* 1993; *Paper* 3/05873E